Unprecedented Pt−Pt Bonded Trimer $\{[Pt_2Cu_4(C{\equiv}CPh)_8]\}_3$ Showing Unusual Near-Infrared Luminescence

Jonathan P. H. Charmant,[†] Juan Forniés,*[,‡] Julio Gómez,[†,§] Elena Lalinde,*[,§] Rosa I. Merino,[‡] M. Teresa Moreno,[§] and A. Guy Orpen[†]

School of Chemistry, University of Bristol, Bristol, BS8 1TS, U.K., Instituto de Ciencia de Materiales de Aragón, Universidad de Zaragoza-Consejo Superior de Investigaciones Científicas, 50009 Zaragoza, Spain, and Departamento de Química, Universidad de La Rioja, 26001, Logroño, Spain

Received March 23, 1999

The homoleptic high-nuclearity platinum−copper acetylide complex of stoichiometry $[PtCu_2(C{\equiv}CPh)_4]$ crystallizes in at least three different polymorphic forms. Dark violet-green crystals with metallic reflectance have been shown by an X-ray diffraction study to be formed by discrete trimers of an hexanuclear octahedral cluster unit $\{[Pt_2Cu_4(C{\equiv}CPh)_8]\}_3$ stabilized by two unsupported Pt−Pt interactions [2.995(1) Å]. The photoluminescence behavior of this complex which is dramatically influenced by strong axial Pt···Pt interactions either in solid state or in solution (CH_2Cl_2 298, 77 K) has been studied.

For several decades there has been considerable interest in the study of the very unusual and highly anisotropic ground- and excited-state properties of complexes in which metal(d^8)−metal(d^8) interactions are present.[1] Predominant are square-planar d^8 platinum complexes which often form stacked linear chain materials with short Pt···Pt contacts (<3.5 Å).[1e−h,2] In these complexes spectroscopic investigations have revealed that such stacking results in the appearance of a low-energy absorption band, often accompanied by visible luminescence, which displays a strong dependence on the interchain metal−metal separation.[1g,2j] Considerable experimental work[2] and recent theoretical calculations[3] seem to indicate that the structural aspects of the stacking are governed not only by Pt···Pt interactions but also by interligand steric repulsions and interligand charge-transfer bonding.[2m] In fact, often the relatively weak Pt···Pt bonding interactions may be offset by other favorable interactions, as is illustrated by the very rich polymorphism exhibited by Pt(II) diimine compounds[2m] [e.g., Pt···Pt in $[Pt(bipy)Cl_2]$ red (3.45 Å),[4a] yellow (4.44 Å)[4b]]. In other cases, these metal−metal or ligand−ligand ($\pi-\pi$) interactions are so enhanced that complexes oligomerize in solution, leading to supramolecular architectures with characteristic photophysical properties.[4c] However, it has been noted that the electronic properties of the ligands have a primary effect on the strength of Pt···Pt bonding, with stronger-field and π-acidic ligands enhancing the interactions of stacked complexes.[2m,3] In fact the shortest M−M distances are found in complexes with ligands such as diimine,[2l] CO,[2h,3,5] CN^-,[1g] or CNR.[3] The alkynyl ligand ($C{\equiv}CR$) bears some similarity (it is a potent σ-donor, but the π-acceptor bonding component is not very important) to the isoelectronic CN^-, CO, or CNR ligands; however related stacked complexes with this ligand were until now unknown.

We report here a new class of aggregates which are based on discrete trimers of a hexanuclear octahedral platinum−copper alkynyl cluster $\{[Pt_2Cu_4(C{\equiv}CPh)_8]\}_3$,

[†] University of Bristol.
[‡] Universidad de Zaragoza-Consejo Superior de Investigaciones Científicas.
[§] Universidad de La Rioja.

(1) (a) For example see: *Extended Linear Chain Compounds*; Miller, J. S., Ed.; Plenum Press: New York, 1982; Vols. 1−3. (b) Miller, J. S.; Epstein, A. J. *Prog. Inorg. Chem*. **1976**, *20*, 1. (c) Mann, K. R.; Lewis, N. S.; Williams, R. M.; Gray, H. B.; Gordon, J. G. *Inorg. Chem*. **1978**, *17*, 828. (d) Finnis, G. M.; Canadell, E.; Campana, Ch.; Dumbar, K. R. *Angew. Chem., Int., Ed. Engl*. **1996**, *35*, 2772, and references therein. (e) Zipp, A. P. *Coord. Chem. Rev*. **1988**, *84*, 47. (f) Krogmann, K. *Angew. Chem., Int. Ed. Engl*. **1969**, *8*, 35. (g) Gliemann, G.; Yersin, H. *Struct. Bonding* **1985**, *62*, 87. (h) Houlding, V. H.; Miskowski, V. M. *Coord. Chem. Rev*. **1991**, 111. (i) Crosby, G. A.; Kendrick, K. R. *Coord. Chem. Rev*. **1998**, *171*, 407.

(2) For recent works see the following references and references therein: (a) Kunkely, H.; Vogler, A. *J. Am. Chem. Soc*. **1990**, *112*, 5625. (b) Connelly, N. G.; Grossley, J. G.; Orpen, A. G.; Salter, H. *J. Chem. Soc., Chem. Commun*. **1992**, 1564 and 1568. (c) Miskowski, V. M.; Houlding, V. H. *Inorg. Chem*. **1991**, *30*, 4446. (d) Yip, H.-K.; Che, Ch.-M.; Zhou, Z.-Y.; Mak, T. C. W. *J. Chem. Soc., Chem. Commun*. **1992**, 1369. (e) Arena, G. Scolaro, L. M.; Pasternack, R. F.; Romeo, R. *Inorg. Chem*. **1995**, *34*, 2994. (f) Bailey, J. A.; Hill, M. G.; Marsh, R. E.; Miskowski, V. M.; Schaefer, W. P.; Gray, H. B. *Inorg. Chem*. **1995**, *35*, 4591. (g) Connick, W. B.; Henling, L. M.; Marsh, R. E. *Acta Crystallogr*. **1996**, *B52*, 817. (h) Bagnoli, F.; Dell'Amico, D. B.; Calderazzo, F.; Englert, U.; Marchetti, F.; Herberich, G. E.; Pascualetti, N.; Ramello, S. *J. Chem. Soc., Dalton Trans*. **1996**, 4317. (i) Palmans, R.; MacQueen, D. B.; Pierpont, C. G.; Fank, A. J. *J. Am. Chem. Soc*. **1996**, *118*, 12647. (j) Connick, W. B.; Henling, L. M.; Marsh, R. E.; Gray, H. B. *Inorg. Chem*. **1996**, *35*, 6261. (k) Daws, Ch. A.; Exstrom, Ch. L.; Sowa, J. R., Jr.; Mann, K. R. *Chem. Mater*. **1997**, *9*, 363. (l) Zheng, G. Y.; Rillema, D. P. *Inorg. Chem*. **1998**, *37*, 1392. (m) Connick, W. B.; Marsh, R. E.; Schaefer, W. P.; Gray, H. B. *Inorg. Chem*. **1997**, *36*, 913. (n) Buss, C. E.; Anderson, C. E.; Pomije, M. K.; Lutz, C. M.; Britton, D.; Mann, K. R. *J. Am. Chem. Soc*. **1998**, *120*, 7783.

(3) Aullón, G.; Alvarez, S. *Chem. Eur. J*. **1997**, *3*, 655.

(4) (a) Osborn, R. S.; Rogers, D. *J. Chem. Soc., Dalton Trans*. **1974**, 1002. (b) Bielli, E.; Gidney, P. M.; Gillard, R. D.; Heaton, B. T. *J. Chem. Soc., Dalton Trans*. **1974**, 2133, and references therein. (c) Arena, G.; Calogero, G.; Campagna, S.; Scolaro, L. M.; Ricevuto, V.; Romeo, R. *Inorg. Chem*. **1998**, *37*, 2763, and references therein.

(5) Chen, Y.-H.; Merkert, J. W.; Murtaza, Z.; Woods, C.; Rillema, D. P. *Inorg. Chim. Acta* **1995**, *240*, 41.

10.1021/om9902030 CCC: $18.00
Publication on Web 07/24/1999

[**1**]$_3$, stabilized by relatively strong unsupported Pt−Pt interactions [2.995(1) Å]. In addition, this complex is a new member of the very select group of transition metal complexes that emit in the near-infrared region of the spectrum.[2k,6]

Some years ago we reported the synthesis of several homoleptic heteropolynuclear platinum alkynyl complexes which, on the basis of a crystal diffraction study on [$Pt_2Ag_4(C{\equiv}CBu^t)_8$], were formulated as hexanuclear derivatives of the type [$Pt_2M_4(C{\equiv}CR)_8$] (M = Cu, Ag, Au; R = Bu^t, Ph).[7] At that time we were intrigued by the fact that while complexes with R = Bu^t were obtained as pale-yellow microcrystalline solids in a low-moderate yield due to their high solubility even in solvents such as diethyl ether or *n*-hexane, complexes with R = Ph could be easily precipitated as deep-yellow (Ag) or red (Cu) solids in high yield by addition of acetone to concentrated dichloromethane or chloroform solutions. We later observed that the color of the phenylacetylide derivatives are highly dependent on the conditions used in the precipitation.[8] For instance, the copper derivative can be obtained as a very dark violet-green solid if the initial solution (CH_2Cl_2, $CHCl_3$) is completely vacuum-dried and then treated with precipitating solvents (acetone, *n*-hexane, MeOH, or EtOH). Moreover, slow diffusion of *n*-hexane into a saturated dichloromethane solution of the complex invariably yields dark violet-green crystals with an intense green metallic reflectance. However, by using less concentrated solutions both red and violet-green crystals may be separated. To further complicate the picture, both the red and green solids turned yellow when stirred with acetonitrile, and a yellow microcrystalline form of this complex which also analyzes as [$PtCu_2(C{\equiv}CPh)_4$] is easily obtained by stirring a chloroform/acetonitrile ($CHCl_3$/MeCN ≈ 1:1) solution of the crude material **1**. To date, all attempts to obtain yellow crystals suitable for X-ray diffraction studies have been unsuccessful. For the silver homologue only yellow (major component) and red (minor component) crystalline forms separated even from very concentrated ($CHCl_3$/*n*-hexane) systems. The crystalline yellow form of the silver derivative contains discrete [$Pt_2Ag_4(C{\equiv}CPh)_8$], but a preliminary X-ray diffraction study of its red form indicates the presence of two octahedral clusters linked by Pt···Pt interactions (3.23 Å).[9] A similar geometry could be assumed for the red polymorph of the copper compound [**1**]$_2$, and the very dark color of the third form prompted us to carry out a structural investigation.

As can be seen (Figure 1), the structure of this dark violet-green polymorph consists of three octahedral hexanuclear [$Pt_2Cu_4(C{\equiv}CPh)_8$] cluster units ([**1**]$_3$) linked

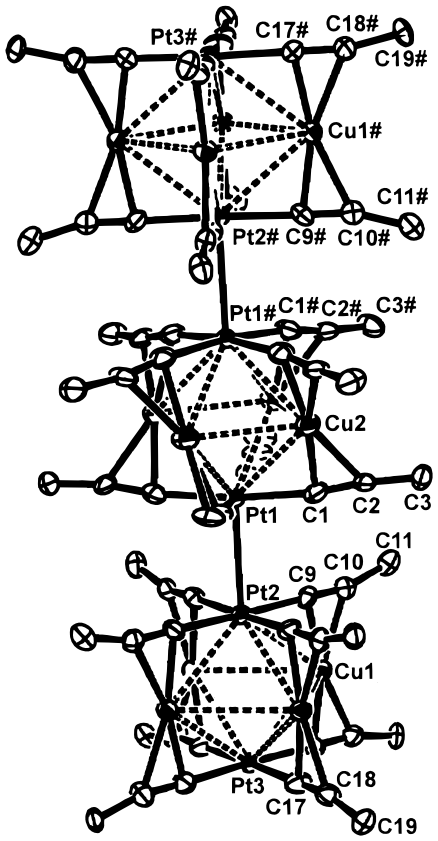

Figure 1. Molecular structure of {[$Pt_2Cu_4(C{\equiv}CPh)_8$]}$_3$, [**1**]$_3$·2CH_2Cl_2. The Ph groups are omitted for clarity.

by two unsupported Pt−Pt bonds. The trimer has exact crystallographic D_4 symmetry, as does the central [$Pt_2Cu_4(C{\equiv}CPh)_8$] unit, while the outer [$Pt_2Cu_4(C{\equiv}CPh)_8$] units have approximate D_{4h} and exact C_4 symmetry. The formal oxidation state of the platinum atoms is +2 and of the copper atoms +1, as in the other polymorphs. The Pt···Pt distance between the clusters **1** within the trimer [2.995(1) Å] is shorter than those seen in the linear-chain Pt(II) complexes (range 3.01−3.50 Å)[1−3] mentioned above and only slightly longer than that found for [$Pt_2(P_2O_5H_2)_4]^{2-}$ [2.9255(1) Å],[1e,10a] for which a very rich photochemistry has been reported.[1e,10b] The reason for the lack of a more extended stacked structure is unclear, but a stereoscopic view of the unit cell clearly indicates the lack of interactions between adjacent trimers (Pt···Pt separation 14.90 Å) (Figure 2). Crystallization solvent (2 mol of CH_2Cl_2 per trimer) does not interact with any of the Pt centers. A remarkable feature of the trimer is the orientation of the Pt_2Cu_4 clusters with respect to each other and also the orientation (eclipsed or staggered) of the two square-planar [Pt(C≡CPh)$_4$] fragments within the octahedral clusters. Thus, whereas the central Pt_2Cu_4 cluster has the same coordination geometry around the metal atoms as [$Pt_2Ag_4(C{\equiv}CBu^t)_8$],[7] with both [Pt(C≡CPh)$_4$] moieties staggered [torsion angle C(1)−Pt(1)−Pt(1)#5−C(1)#5 38°], the external octahedral clusters exhibit essentially eclipsed disposition of the [Pt(C≡CPh)$_4$] units [torsion angle C(17)−Pt(3)−Pt(2)−C(9) 1°]. On the other hand, as is typical for stacked d^8−d^8 complexes, the C≡CPh

(6) (a) Pelletier, Y.; Reber, Ch. *Inorg. Chem.* **1997**, *36*, 721. (b) Richter, M. M. *Inorg. Chem.* **1993**, *35*, 5762. (c) Juris, A.; Bolzani, V.; Campagna, S.; Denti, G.; Serroni, S.; Frei, G.; Güdel, H. U. *Inorg. Chem.* **1994**, *33*, 1491. (d) Bilsel, O.; Rodriguez, J.; Milam, S. N.; Gorlin, P. A.; Girolami, G. S.; Suslik, K. S.; Holten, D. *J. Am. Chem. Soc.* **1992**, *114*, 6528. (e) Balch, A. L.; Nagle, J. K.; Olmstead, M. M.; Reedy, P. E., Jr. *J. Am. Chem. Soc.* **1987**, *109*, 4123.

(7) Espinet, P.; Forniés, J.; Martínez, F.; Tomás, M.; Lalinde, E.; Moreno, M. T.; Ruiz, A. J.; Welch, A. J. *J. Chem. Soc., Dalton Trans.* **1990**, 791.

(8) (a) Forniés, J.; Lalinde, E.; Martín, A.; Moreno, M. T. *J. Organomet. Chem.* **1995**, *490*, 179. (b) Ara, I.; Gómez, J.; Forniés, J.; Lalinde, E.; Merino, R. I.; Moreno, M. T. *Inorg. Chem. Commun.* **1999**, *2*, 62.

(9) Unpublished results due to unresolved crystallographic problems with the red form.

(10) (a) Marsh, R. E.; Herbstein, F. H. *Acta Crystallogr., Sect. B* **1983**, *39*, 280. (b) Roundhill, D. M.; Gray, H. B.; Che, C.-M. *Acc. Chem. Res.* **1989**, *22*, 55 and references therein.

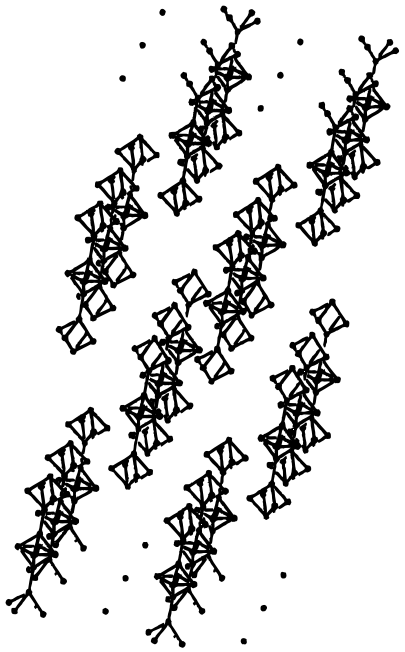

Figure 2. Stereoscopic view of the packing of{[Pt_2Cu_4(C≡CPh)$_8$]}$_3$, [**1**]$_3$·2CH_2Cl_2.

ligands of the corresponding square-planar platinum environments of the platinum atoms which define the shorter Pt−Pt distance adopt a staggered orientation so that the Pt_2Cu_4 octahedra are successively twisted by 44°. The Pt−Cu distances [$(Pt_2Cu_4)_{central}$ 2.918(1) Å and $(Pt_2Cu_4)_{external}$ 3.027(1) and 3.020(1) Å] are comparable with those seen in the related derivative [1,1-ferrocenediyl Pt_2Cu_3(C≡CPh)$_6$] [2.845(5), 2.975(3) Å][11] but closer to the sum of van der Waals radii (Pt···Cu 3.15 Å),[12] suggesting only very weak interactions. However, the Cu−Cu distances [$(Pt_2Cu_4)_{central}$ 3.031(2), $(Pt_2Cu_4)_{external}$ 3.301 Å] are larger than the separation in metallic copper (2.56 Å) or the sum of the van der Waals radii of two Cu atoms (2.8 Å),[12] ruling out any bonding interaction.

Presumably the η^2-acetylenic-copper interactions [range Cu−C_α 1.982(8)−1.995(7) Å; Cu−C_β 2.137(8)−2.158(8) Å] play an essential role in the trimer formation, enhancing the Pt−C_α π-acceptor bonding component, which decreases the electron density on platinum, thereby reducing electronic repulsions between the Pt centers and favoring Pt−Pt bonding interactions between clusters. In addition the electrostatic interactions between the Cu(I) and $[Pt(C{\equiv}CR)_4]^{2-}$ centers may be an important factor in the stability of the octahedral clusters **1**.

By analogy with previous reports,[1e−h,2] the colors of the different polymorphs can be taken to be related to the degree of oligomerization in the solid state and presumably to the variation of intercluster metal−metal separations (yellow form of **1** > red [**1**]$_2$ > dark violet-green [**1**]$_3$). In the solid state electronic interactions between clusters are clearly observed in the trimeric dark violet-green form as a moderately broad absorption band around 621 nm. The absence of this band in the spectrum of the dissolved crystals (CH_2Cl_2 ≈10^{-4} M) together with the loss of color, forming a yellow solution, implies that it is associated with solid-state effects. Therefore we attributed the intense color to the low-energy transition that arises as a consequence of Pt−Pt interactions in the trimer [**1**]$_3$.

Before the luminescence behavior of this cluster is discussed (see Table 2), it should be noted that the homoleptic $(NBu_4)_2$[Pt(C≡CPh)$_4$] precursor is slightly emissive in the solid state at room temperature, exhibiting a vibronic structural band at ca. 447 nm with vibrational progressional spacing of ca. 2045−2080 cm^{-1} characteristic of the ν(C≡C) mode. On the basis of previous spectroscopic studies with neutral alkynyl platinum complexes,[13] this emission can be assigned to a π^*/pz → d_{z^2} transition (MLCT). Excitation maxima for this emission are observed at 423, 392, and 361 nm. The emission of the platinum−copper cluster depends on its polymorphic form. Thus, in solid state at room temperature excitation of the dark violet-green form {[Pt_2Cu_4-(C≡CPh)$_8$]}$_3$, [**1**]$_3$, (KBr pellets) with different excitation wavelengths in the visible range (435 and 627 nm) produces a long-lived (lifetime 0.5 μs) very strong near-infrared luminescence as a structureless symmetric band with a λ_{max} at 806 nm (12406 cm^{-1}; hwhm of 1970 cm^{-1}) (Figure 3). The excitation spectrum of this emission displays two excitation maxima at 430 and 625 nm, thus reflecting prominently the solid-state absorption

Table 1. Selected Bond Lengths (Å) and Angles (deg) for {[Pt_2Cu_4(C≡CPh)$_8$]}$_3$, [1**]$_3$·2CH_2Cl_2**

Pt(1)−C(1)	2.014(9)	Pt(1)−Cu(2)	2.918(1)
Pt(1)−Pt(2)	2.995(1)	Pt(2)−C(9)	2.012(7)
Pt(2)−Cu(1)	3.027(1)	Pt(3)−C(17)	1.994(8)
Pt(3)−Cu(1)	3.020(1)	Cu(1)−C(17)	1.982(8)
Cu(1)−C(9)	1.995(7)	Cu(1)−C(18)	2.158(8)
Cu(1)−C(10)	2.153(8)	Cu(2)−C(1)	1.990(8)
Cu(2)−C(2)	2.137(8)	Cu(2)−Cu(2)#1[a]	3.031(2)
C(1)−C(2)	1.240(11)	C(2)−C(3)	1.401(11)
C(9)−C(10)	1.207(10)	C(10)−C(11)	1.453(11)
C(17)−C(18)	1.244(11)	C(18)−C(19)	1.438(10)
Pt(1)−C(1)−C(2)	171.9(6)	C(1)−C(2)−C(3)	169.6(9)
Pt(2)−C(9)−C(10)	1784(8)	C(9)−C(10)−C(11)	164.4(8)
Pt(3)−C(17)−C(18)	178.4(8)	C(17)−C(18)−C(19)	167.2(8)
C(1)−Pt(1)−Pt(2)	93.4(2)	C(9)−Pt(2)−Pt(1)	88.8(2)

[a] Symmetry transformations used to generate equivalent atoms: #1 y, $-x+1/2$, z.

Table 2. Emission Spectral Data for [Pt_2Cu_4(C≡CPh)$_8$], 1, [Pt_2Cu_4(C≡CBu^t)$_8$], [Pt_2Ag_4(C≡CPh)$_8$], and $(NBu_4)_2$[Pt(C≡CPh)$_4$]

compd	medium (temp/K)	λ_{max}^{em}/nm
[**1**]$_3$	solid state, KBr (298)	806
[**1**]$_2$	solid state, KBr (298)	715
1	yellow solid	550
	CH_2Cl_2, 10^{-2} M (298)	707
	CH_2Cl_2, 10^{-2} M (77)	827
	CH_2Cl_2, 10^{-3} M (298)	710
	CH_2Cl_2, 10^{-3} M (77)	818
	CH_2Cl_2, 10^{-4} M (77)	815
	CH_2Cl_2, 5×10^{-5} M (77)	813
	CH_2Cl_2, 2×10^{-5} M (77)	809, 728
	CH_2Cl_2, 10^{-5} M (77)	708
[Pt_2Cu_4(C≡CBu^t)$_8$]	solid state, KBr (298)	583
[Pt_2Ag_4(C≡CPh)$_8$]	solid state, KBr (298)	570
{[Pt_2Ag_4(C≡CPh)$_8$]}$_2$	solid state, KBr (298)	662
$(NBu_4)_2$[Pt(C≡CPh)$_4$]	solid state, KBr (298)	447, 465, 490

(11) Tanaka, S.; Yoshida, T.; Adachi, T.; Yoshida, T.; Onitsuka, K.; Sonogashira, K. *Chem Lett.* **1994**, 877.
(12) Huheey, J. E.; Keiter, E. A.; Keiter, R. A. *Inorganic Chemistry*, 4th ed.; Harper Collins College Publishers: New York, 1993; p 292.
(13) Sacksteder, L.; Baralt, E.; DeGraff, B. A.; Lukehart, C. M.; Demas, J. N. *Inorg. Chem.* **1991**, *30*, 2468.

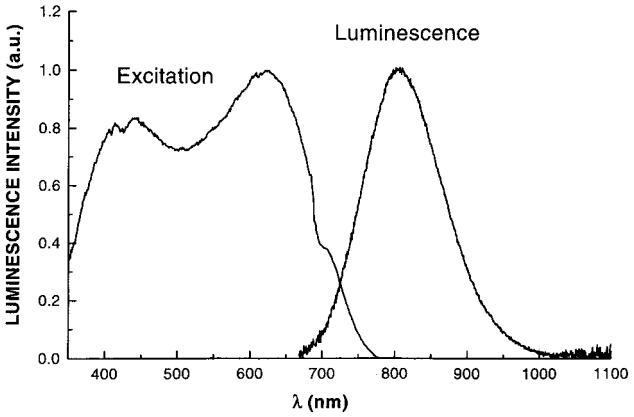

Figure 3. Solid-state emission and excitation of $\{[Pt_2Cu_4(C{\equiv}CPh)_8]\}_3$, $[\mathbf{1}]_3$, at room temperature.

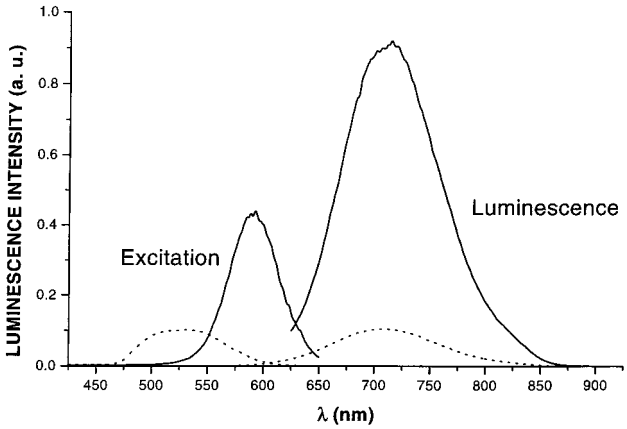

Figure 4. Emission and excitation spectra of $[Pt_2Cu_4(C{\equiv}CPh)_8]$, [**1**], in degassed CH_2Cl_2 at room temperature. 10^{-2} M (—) and 10^{-3} M (- - -).

features seen in the low-energy region (λ > 300 nm). Similarly, the red crystalline form displays a more asymmetric but also intense emission significantly shifted to higher energies ($\lambda^{em}_{max} \approx 715$ nm) with a broad excitation maximum around 475 nm, which tails to longer wavelength. Although the IR spectrum of the yellow form is quite similar [ν(C≡C) 2021(m), 1979(sh) cm^{-1}] to those of the red [ν(C≡C) 2020(m) cm^{-1}] and violet-green [ν(C≡C) 2032, 2022(m) cm^{-1}] forms, the properties of the former are rather intriguing and led us to suspect that it is not a simple monomer. First, once formed the yellow solid is not soluble in solvents such as CH_2Cl_2 or $CHCl_3$, in which the red and violet-green forms are very soluble. On the other hand, this solid is also emissive, showing a structureless asymmetric emission band (with a tail to lower energies) centered at ca. 550 nm with excitation maxima at 397 and 333 nm. Recently, we have reported that the analogous monomer $[Pt_2Ag_4(C{\equiv}CBu^t)_8]$ exhibited an intense luminescence band at 476 nm.[8b] According to previous reports[14] this emission was ascribed to a π^*-(C≡CR) → CC transition (cluster centered to ligand charge transfer), though mixing of p_z (Pt) and π^*(C≡CR) orbitals is symmetry allowed and presumably occurs to some extent. The involvement of alkynyl ligands and of silver metal centers in the LUMO and HOMO orbitals, respectively, is consistent with the red shift observed in the emission of the analogous yellow monomeric derivatives $[Pt_2Ag_4(C{\equiv}CPh)_8]$ (λ^{em}_{max} 570 nm) and $[Pt_2Cu_4(C{\equiv}CBu^t)_8]$ (λ^{em}_{max} 583 nm), respectively (Table 2). Similar observations have been previously observed for related polynuclear platinum (C≡CPh vs $C{\equiv}CBu^t$)[15] copper or silver alkynyl complexes and thiocarbamate clusters of type $[M_6(mtc)_6]$.[16] In this context the emission for the $[Pt_2Cu_4(C{\equiv}CPh)_8]$ monomer should presumably be red shifted relative to those observed for the yellow monomer forms of $[Pt_2Ag_4(C{\equiv}CPh)_8]$ and $[Pt_2Cu_4(C{\equiv}CBu^t)_8]$, respectively, and therefore, the emission observed at 550 nm is at very high energy. Preliminary results also show that the emission properties of this yellow form are dependent on the pressure used to make the solid pellet (with KBr). An increase of the pressure used darkens the sample (from yellow to brown) and is accompanied by the appearance of a low-energy emission and concomitant reduction of the intensity of the high-energy band (for example, for a sample prepared using 9−10 Torr for 3 h, two maxima at ca. 563 and 758 nm are observed). The low-energy emission can be tentatively ascribed to the formation of aggregates (dimers or trimers). In fact we have also observed that if the yellow solid is vigorously stirred, over 24 h it turns green, and the trimer form of the cluster may be isolated in 70% yield from this solid by treatment with CH_2Cl_2 and usual workup. The dimeric red crystalline polymorph[9] of the phenylacetylide silver−platinum complex $\{[Pt_2Ag_4(C{\equiv}CPh)_8]\}_2$ also exhibits a slightly asymmetric emission, at higher energy (λ^{em}_{max} 662 nm) than that seen for the red $\{[Pt_2Cu_4(C{\equiv}CPh)_8]\}_2$ form (see Table 2), as might be expected.

The notable displacement to lower frequencies from monomer to dimer and from dimer to trimer of the observed luminescence for the cluster platinum−copper complex suggests a strong perturbation due to axial Pt···Pt interactions. According to previous observations[1,2c,j,l,m] metal−metal interactions can greatly increase the energy of the dσ^* combination of d_{z^2} orbitals involved in the HOMO and decrease the energy of the corresponding $p_z\sigma$ combination of the p_z orbitals involved in the LUMO, which should clearly lower the energy of the emission relative to the monomer. In linear chain platinum complexes, this effect is enhanced by shorter Pt−Pt distances, and therefore, a weaker Pt···Pt interaction is suggested in the red form $[\mathbf{1}]_2$ relative to that seen for the dark violet-green form $[\mathbf{1}]_3$.

In solution of CH_2Cl_2 at room temperature the phenylacetylide Pt_2Cu_4 complex **1** shows an emission that varies with concentration. Thus at low concentrations (less than 10^{-3} M) the solutions are yellow and the luminescence is lost or cannot be detected. However, upon increasing the concentration, the solution turns deep-orange and a red emission around 710 nm appeared, whose intensity gradually grew with the concentration (see Figure 4). The very low energy of this emission and the sharpness of the excitation band with a λ^{ex}_{max} at 592 nm (for a solution of 10^{-2} M) suggest that it can be attributed to the presence of dimers in solution

(14) Yam, V. W.-W. *Photochem. Photobiol. A*: *Chem.* **1997**, *106*, 75.
(15) (a)Yam, V. W.-W.; Chan L.-P.; Lai, T. F. *Organometallics* **1993**, *12*, 2197. (b) Yam, V. W.-W.; Fung, W. K.-M.; Cheung, K.-K. *Organometallics* **1997**, *16*, 2032. (c) *Ibid. J. Chem. Soc., Chem. Commun.* **1997**, 963.
(16) (a) Sabin, F.; Ryu, C. K.; Ford, P. C.; Vogler, A. *Inorg. Chem.* **1992**, *31*, 1941. (b) Ford, P. C.; Vogler, A. *Acc. Chem. Res.* **1993**, *26*, 220.

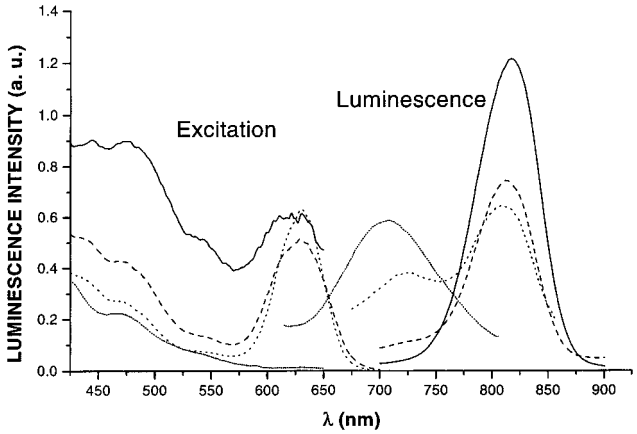

Figure 5. Emission and excitation spectra of $[Pt_2Cu_4(C{\equiv}CPh)_8]$, [**1**], in degassed CH_2Cl_2 at 77 K. 10^{-3} M (—), 5×10^{-5} M (– – –), 2×10^{-5} M (- - -), and 10^{-5} M (···).

bonded by a Pt−Pt interaction. The room-temperature solutions of **1** are not emissive when excited with light of low wavelengths ($\lambda < \sim 500$ nm), suggesting that probably monomers do not luminesce and that Pt−Pt interactions have to exist in order to observe luminescence. Therefore, the emission has presumably more pronounced platinum-centered character (Pt−Pt $d\sigma^* \rightarrow p_z\sigma$).

The emission spectrum at 77 K (CH_2Cl_2) also undergoes a considerable change with the concentration (Figure 5). At concentrations [**1**] $> 5 \times 10^{-5}$ M only a low-energy emission is observed (827−813 nm, Table 2) which is 4 or 5 times more intense, somewhat narrower, and considerable red shifted from that seen in solution at 298 K (for solutions with [**1**] $> 10^{-3}$ M). A decrease of the concentration was accompanied by the appearance of a high-energy emission (λ^{em}_{max} 708 nm) and a concomitant reduction of the low-energy band, which is finally lost at a very low concentration (10^{-5} M). The excitation spectra are also highly dependent on concentration, showing a distinctly prominent maximum at ca. 630 nm only monitoring the low-energy band. It was found that when yellow or deep-orange (CH_2Cl_2) solutions ([**1**] $> 2 \times 10^{-5}$ M) of complex **1** are frozen, the glasses are green (and saturated solutions are very dark). This fact and the observation of two emissions at intermediate concentrations (2×10^{-5} M, 809, 728 nm) in fluid solution at low temperature (77 K) suggest the existence of two self-trapped states of two emitting species. The low-energy band is very near to that observed for the dark violet-green form in the solid state, implying the presence of aggregates (trimers) formed as the solution cools. The emission observed at very low concentration (708 nm) is very near that seen for the red solid (715 nm) and may be tentatively attributed to the presence of dimers.

This type of high-nuclearity heteronuclear alkynyl complexes possess interesting properties for study, including an intense near-infrared luminescence and tendency to oligomerize both in solid state and in solution. The results discussed above indicate the importance of η^2-acetylenic bonding interactions in these properties. Thus, the possibility of performing a fine-tuning of these properties by varying the substituent alkynyl groups and the metal center implicated in the η^2-interactions makes the synthesis and the study of these compounds very interesting.

Experimental Section

The optical absorption spectra were recorded using a Hewlett-Packard 8453 (solution) spectrophotometer in the visible and near-UV ranges. Luminescence and excitation spectra were recorded using a Perkin-Elmer luminescence spectrometer LS 50B with red sensitive photomultiplier type R928 or photomultiplier (VIS)/Si photodiode (near-IR) (luminescence) and a standard calibrated xenon lamp of 1000 W (excitation). The lifetime was measured using a pulsed EG&G dye laser. The complexes $(NBu_4)_2[Pt(C{\equiv}CPh)_4]$ and $[Pt_2M_4(C{\equiv}CR)_8]$ (M = Cu, Ag; R = Ph, Bu^t) were prepared as we described elsewhere.[7] Solutions for photochemical experiments were prepared using CH_2Cl_2 previously distilled over CaH_2 and degassed by at least four freeze−pump−thaw cycles.

Slow diffusion of *n*-hexane into a saturated CH_2Cl_2 solution (red-garnet) of the complex $[Pt_2Cu_4(C{\equiv}CPh)_8]$ **1** yields dark violet-green crystals with metallic reflectance $[\mathbf{1}]_3$ suitable for X-ray diffraction and luminescence studies. However if less concentrated solutions (orange) are used, a mixture of red $[\mathbf{1}]_2$ (used for luminescence studies) and dark violet-green $[\mathbf{1}]_3$ crystals is obtained.

Stirring a yellow solution of **1** in a $CHCl_3/CH_3CN$ mixture (~1:1) affords a yellow microcrystalline precipitate (yellow form), which also analyzes as $[PtCu_2(C{\equiv}CPh)_4]$.

A yellow microcrystalline sample of $[Pt_2Ag_4(C{\equiv}CPh)_8]$ for luminescence studies was prepared by slow diffusion of *n*-hexane into a CH_2Cl_2 solution of the complex. Red crystals of $\{[Pt_2Ag_4(C{\equiv}CPh)_8]\}_2$ were only obtained by diffusion of *n*-hexane into a $CHCl_3$ solution of complex $[Pt_2Ag_4(C{\equiv}CPh)_8]$ (together with yellow crystals), which were separated by hand for luminescence studies.

X-ray Diffraction Study of $[\mathbf{1}]_3{\cdot}2CH_2Cl_2$. Crystallographic data: empirical formula $Pt_6Cu_{12}Cl_4C_{194}H_{124}$, tetragonal, space group *P*4/*nnc* (No. 126), $a = 16.143(2)$ Å, $c = 32.538(3)$ Å, $V = 8479.3(16)$ Å^3 $Z = 2$, $\mu = 6.509$ mm^{-1}, crystal dimensions $0.50 \times 0.40 \times 0.40$ mm. All diffraction measurements were made at −100 °C with a Siemens three-circle SMART[17] area detector diffractometer using graphite-monochromated Mo Kα radiation and intensities integrated using the SAINT[18] program. No crystal decay was observed over the data collection period. A total of 50579 diffracted intensities were measured in a hemisphere of reciprocal space ($1.25° < \theta < 27.49°$); 4877 unique observations remained after averaging of duplicate and equivalent measurements (R_{int} 0.057) and deletion of the systematic absences. Of these 3393 had $I > 2\sigma(I)$. The data were processed by SADABS;[19] effective transmission coefficients were in the range 0.403−0.264. Lorentz and polarization corrections were also applied.

The structure was solved by direct methods and refined using full-matrix least-squares refinement on F^2 with the SHELXL-97 program.[20] All hydrogen atoms (except solvent hydrogens, which were not included in the model) were constrained to idealized geometries and assigned isotropic displacement parameters 1.2 times the U_{iso} value of their attached carbon for the aromatic hydrogens. Phenyl rings showed two disorders corresponding to rotation about the $C_{ipso}{\cdots}C_{para}$ axis. Refinement of the 364 least-squares variables converged to residual indices [$I > 2\sigma(I)$]: R1 = 0.0503, wR2 = 0.1342, $S = 1.662$*. Weights, *w*, were set equal to $1/[\sigma^2(F_o^2) +$

(17) *SMART* (Siemens Molecular Analysis Research Tool); Siemens Analytical X-ray: Madison, WI, 1989−1995.
(18) *SAINT* (Siemens Area Detector Integration) program; Siemens Analytical X-ray: Madison, WI, 1995.
(19) Sheldrick, G. *SADABS* (Siemens Area Detector Absorption); University of Göttingen: Germany, 1996.
(20) *SHELXTL*, Rev. 5.0,3; Siemens Analytical X-ray: Madison, WI, 1994.

$(gP)^2 + dP]^{-1}$, where $P = [\max(F_o^2,0) + 2F_c^2]/3$ and $g = 0.05$, and were set to minimize the variation in S as a function of $|F_o|$. Final difference electron density maps showed no features outside the range 1.34 to −1.61 e Å^{-3}, the largest being close to a platinum atom.

Acknowledgment. We thank the Dirección General de Enseñanza Superior (Spain, Projects PB95-0003C02-01 02) and the University of La Rioja (Project API-99/B17 and a grant to J.G.) for financial support.

Supporting Information Available: X-ray experimental data for [**1**]$_3$ including tables of positional parameters and anisotropic thermal parameters. This material is available free of charge via the Internet at http://pubs.acs.org.

OM9902030